horticulturae

MDPI

Article

The Heavy Metal-Associated Isoprenylated Plant Protein (HIPP) Gene Family Plays a Crucial Role in Cadmium Resistance in Lotus (*Nelumbo nucifera* G.)

Chunyan Gao [1,2], Yuxuan Zhu [1], Hualei Xu [3], Xinyue Peng [1], Kaili Yu [4], Xi Gu [5], Yan Xiao [5], Jian Cai [1] and Yinjie Wang [5,*]

[1] School of Biology and Food Engineering, Fuyang Normal University, Fuyang 236037, China
[2] Fuyang Normal University—Funan Rural Revitalization Collaborative Technology Service Center, Fuyang Normal University, Fuyang 236037, China
[3] School of History, Culture and Tourism, Fuyang Normal University, Fuyang 236037, China
[4] State Key Laboratory of Crop Genetics and Germplasm Enhancement and Utilization, Nanjing Agricultural University, Nanjing 210095, China
[5] Institute of Botany, Jiangsu Province and Chinese Academy of Sciences, Nanjing 210014, China
* Correspondence: wyinjie89@126.com; Tel.: +86-25-84347086

Abstract

Cadmium (Cd) contamination poses significant threats to aquatic ecosystems. Heavy metal-associated isoprenylated plant proteins (HIPPs) are plant-specific chaperones involved in metal ion homeostasis and stress adaptation. Lotus is an aquatic plant with high biomass and Cd accumulation capacity, showing great potential in water remediation. However, the functional characterization of *HIPPs* in lotus remains unexplored, limiting its application in phytoremediation. We conducted comprehensive characterization of *NnHIPP* genes in lotus, integrating comparative genomics, Cd-stress transcriptomics, and heterologous expression assays in transgenic yeast. This study identified 33 *NnHIPP* genes classified into five subfamilies with conserved motifs and structures. Synteny analysis revealed closer evolutionary relationships with dicots (*Arabidopsis* and *Medicago sativa*) than monocots. Abundant stress-responsive elements were found in *NnHIPPs* promoters. Tissue-specific expression profilings indicated functional diversification across organs and developmental stages. Our transcriptome analysis revealed that most *NnHIPPs* responded to Cd stress, with stronger induction in roots than leaves. Four Cd-induced NnHIPPs (NnHIPP10/14/21/33) showed both plasma membrane and nuclear localization. Notably, NnHIPP14, NnHIPP21, and NnHIPP33 conferred varying degrees of Cd tolerance when overexpressed in yeast. Our study demonstrates that *NnHIPPs* participate in Cd stress response. Three candidate *NnHIPP* genes are proposed for genetic engineering to enhance phytoremediation efficiency in lotus.

Keywords: lotus; HIPP; Cd; phytoremediation

Academic Editor: Sergey V. Dolgov

Received: 9 August 2025
Revised: 4 September 2025
Accepted: 16 September 2025
Published: 18 September 2025

Citation: Gao, C.; Zhu, Y.; Xu, H.; Peng, X.; Yu, K.; Gu, X.; Xiao, Y.; Cai, J.; Wang, Y. The Heavy Metal-Associated Isoprenylated Plant Protein (HIPP) Gene Family Plays a Crucial Role in Cadmium Resistance in Lotus (*Nelumbo nucifera* G.). *Horticulturae* **2025**, *11*, 1136. https://doi.org/10.3390/horticulturae11091136

1. Introduction

Rapid urbanization and industrialization have increased heavy metal pollution in water worldwide. Industrial wastewater, metal smelting, and improper sewage disposal are key contributors. Agricultural irrigation with contaminated water further introduces heavy metals into farmland soils, thereby posing a serious threat to food safety and human health. Among various heavy metals, Cd is particularly concerning due to its high toxicity, environmental mobility, and potential for bioaccumulation [1,2]. As a non-essential element

in plants, Cd exerts multifaceted detrimental effects on plant physiology and development. Cd preferentially accumulates in root tissues, where it impairs meristematic activity and alters root system architecture, ultimately compromising nutrient acquisition [3]. Subsequent translocation to aerial tissues disrupts photosynthetic machinery through both structural damage to chloroplasts and functional interference with electron transport chains [4]. These physiological disruptions are compounded by Cd-induced oxidative stress, which overwhelms cellular antioxidant defenses and leads to lipid peroxidation, protein denaturation, and DNA damage [5,6]. Reproductive development is particularly vulnerable; Cd exposure adversely affects seed set and fruit quality in plants and male infertility in aquatic animals [7]. These collective impairments result in stunted growth, diminished biomass, and decreased crop yield, underscoring the urgent need for effective remediation strategies [8]. Remediating Cd-contaminated water is therefore very important. Phytoremediation, which utilizes plants to uptake and transport heavy metals, offers a promising solution due to its low cost, environmental friendliness, and minimal secondary pollution [9,10]. Consequently, phytoremediation is now a major research focus for ecological restoration in water bodies.

Using ornamental plants for remediation is especially promising. These plants can remove pollutants while also improving the landscape [4,11]. Lotus (*Nelumbo nucifera* G.), a central element in waterscape garden design, ranks among China′s top ten traditional ornamental flowers [12]. It holds significant cultural, economic, and ornamental value [13,14]. Lotus exhibits remarkable heavy metal phytoremediation potential, with an 85% Cd removal efficiency from water [15,16]. Its rapid growth and high biomass further support its utility for remediating Cd-contaminated waters. However, the molecular mechanisms underlying Cd tolerance in lotus remain unclear, limiting its large-scale application in phytoremediation. Therefore, enhanced characterization of Cd-responsive genes in *Nelumbo nucifera* is critical for improving Cd tolerance.

HIPPs are important metal chaperones that regulate ion uptake, translocation, and compartmentalization, thereby alleviating metal-induced cellular stress. HIPP proteins feature two conserved motifs: an N-terminal CysXXCys (X = any amino acid) sequence within the HMA domain and a C-terminal CaaX prenylation motif. The unique combination of one or two HMA domains and prenylation modification distinguishes HIPPs as plant-exclusive proteins [17]. Functionally, HIPPs mediate both developmental processes and stress adaptation, including responses to pathogens and abiotic challenges such as cold, drought, and heavy metal toxicity [18]. Recent studies demonstrate that silencing *NbHIPP3*, the homolog of citrus *HIPP03* in the *Nicotiana benthamiana*, significantly enhances plant resistance against *Pseudomonas syringae* infection [19]. HIPP1-V has been identified as a positive regulator of powdery mildew resistance in wheat by inhibiting the pathogen *haustorium's* development. Both transient and stable overexpression of *HIPP1-V* in wheat conferred enhanced resistance to powdery mildew [20]. In terms of abiotic stress, AtHIPP3 participates in the ABA signaling regulatory network of *Arabidopsis thaliana* in response to drought stress, and its expression level is downregulated under stress [21]. The sorghum *SbHIPP40* overexpression not only restored Cd tolerance in *ycf1* mutants but also increased Cd accumulation in aerial tissues of transgenic rice compared to wild-type plants [22]. After overexpressing alfalfa *HIPP12*, the Cd tolerance of transgenic Arabidopsis is positively regulated through reduced Cd accumulation, improved antioxidant capacity, and sustained photosynthesis [23]. Overexpression of *Camellia sinensis CsHIPP22*, *CsHIPP24*, or *CsHIPP36* confers enhanced Cd stress resistance in the Cd-sensitive *ycf1* yeast mutant [24]. Knockdown of *ZmHIPP22* significantly impairs maize seedling growth and reduces Pb accumulation under lead (Pb) stress. Researchers have found that ZmHIPP22 conferred tolerance by facilitating Pb deposition in the cell wall, sequestering Pb away from intracellular organelles [25]. OsHIPP29 and OsHIPP24 in rice precisely control the absorption, transport,

and redistribution processes of divalent metal ions Cu^{2+} and Cd^{2+}, respectively [26,27]. In addition, HIPPs coordinate plant environmental adaptation through hormone signal transduction. AtHIPP3 regulates pathogen responses via the salicylic acid pathway, acting as an upstream modulator of plant immunity and flowering time. In abscisic acid (ABA)-mediated Cd accumulation, the core signaling component ABI5 interacts with MYB49 (R2R3-MYB family) to control Cd accumulation by regulating *bHLH38*, *bHLH101*, *HIPP22*, and *HIPP44* expression [28]. Additionally, cytokinin oxidase (CKX) proteins synthesized in the endoplasmic reticulum specifically interact with HIPPs in Arabidopsis, responding to cytokinin negative feedback signals to maintain cellular homeostasis [29].

HIPPs have been proposed as key contributors to Cd detoxification in plants. Nevertheless, systematic investigation of the *HIPP* gene family in *Nelumbo nucifera* is still lacking, and the functional specificity of its members remains poorly defined. Unlike model species such as Arabidopsis or crops like rice and alfalfa, lotus not only exhibits high Cd accumulation capacity and aquatic adaptability but also retains significant landscape value as an ornamental plant, making it an ideal system for studying heavy metal tolerance without compromising aesthetic function. In this study, we performed a genome-wide identification of *HIPP* genes in lotus and characterized their phylogenetic evolution, gene structure, motif composition, chromosomal distribution, tissue-specific expression, and promoter cis-elements. Expression dynamics under Cd stress in leaves and roots were analyzed to uncover responsive candidates. Furthermore, subcellular localization was integrated with heterologous functional assays in yeast to investigate the mechanistic roles of candidate NnHIPPs in enhancing Cd tolerance. This study provides critical insights into the molecular functions of *NnHIPP* genes in Cd detoxification and offers valuable genetic resources for improving phytoremediation capacity in lotus through molecular breeding.

2. Materials and Methods

2.1. Plant Materials and Experimental Treatments

The seeds of lotus "Weishanhuhonglian" were germinated in distilled water and subsequently cultivated under greenhouse conditions at 30 °C/25 °C under 16 h light/8 h dark. Three-week-old seedlings were treated with 5% Hoagland solution (pH 6.0) containing 30 μM $CdCl_2$ for Cd stress [30], while seedlings maintained in 5% Hoagland solution (pH 6.0) alone served as a control [31]. The leaves and roots were collected at 0 h, 3 h, 6 h, 12 h, 24 h, and 48 h after Cd stress treatments, respectively. Each treatment included three biological replicates. After collection, samples were immediately frozen in liquid nitrogen and stored at −80 °C until RNA isolation.

2.2. Identification and Physicochemical Properties of HIPP Genes in Nelumbo nucifera

Genome sequences of *Nelumbo nucifera* were obtained from the Ensembl Plants database (https://plants.ensembl.org/index.html, accessed on 5 April 2025). The protein sequences of HIPP in *Arabidopsis* and rice were downloaded from the PlantTFDB database and Rice Genome Annotation Project, respectively. The hidden Markov model (HMM) for the HMA domain (PF00403) was retrieved from the Pfam database (http://pfam.sanger.ac.uk/, accessed on 7 April 2025), and then used to search the NnHIPP protein sequences in *Nelumbo nucifera* with TBtools (version 2.330) [23]. *Arabidopsis thaliana* HIPP proteins were used as queries to discover homologous genes from lotus using TBtools. Subsequently, the list of homologs was further optimized by confirming the presence of C-terminal prenylation motifs, leading to the final selection of putative *NnHIPP* genes. ExPASy ProtParam tool (https://web.expasy.org/protparam, accessed on 10 April 2025) was used to determine the physicochemical properties of NnHIPPs, while WoLF PSORT II tool

(https://www.genscript.com/wolf-psort.html, accessed on 12 April 2025) was used to predict their subcellular localization [32].

2.3. Phylogenetic Analysis

To explore the evolutionary relationships of HIPP proteins, multiple alignments of HIPP proteins from *Arabidopsis thaliana*, *Oryza sativa*, and *Nelumbo nucifera* were performed using ClustalW tool in MEGA 7.0 software (version 7.0.26) [33]. The phylogenetic tree was inferred by the Neighbor-Joining algorithm with 1000 bootstrap replicates. The phylogenetic tree was subsequently visualized using iTOL (https://itol.embl.de/, accessed on 17 April 2025) [34].

2.4. Structural and Conserved Motif Analysis of NnHIPPs

To explore the structure of *NnHIPP* genes, the CDS (coding sequences) were extracted from GFF file using TBtools. The protein domains of *NnHIPPs* were systematically annotated with the CD search program (https://www.ncbi.nlm.nih.gov/Structure/cdd/wrpsb.cgi, accessed on 6 May 2025). Conserved motifs within the NnHIPP proteins were identified with the MEME online software (version 5.5.8, http://meme-suite.org/, accessed on 8 May 2025), and the exon–intron structures of *NnHIPP* genes were analyzed and visualized using TBtools.

2.5. Chromosome Distribution and Synteny Analysis in NnHIPP Gene Family

The chromosomal locations of *NnHIPP* genes were visualized using TBtools [35]. The genome GFF3 files and FASTA annotation files of *Nelumbo nucifera*, *Arabidopsis thaliana*, *Zea mays*, *Oryza sativa*, and *Medicago sativa* were downloaded from the Ensembl Plants database. Gene duplication events of *NnHIPP* genes in *Nelumbo nucifera* genome were analyzed using MCScanX (JCVI v1.1.7), and synteny maps were generated and visualized via TBtools [36,37].

2.6. Analysis of NnHIPP Cis-Acting Elements

For promoter analysis of *NnHIPPs* in *Nelumbo nucifera*, the 2.0 kb sequences upstream of ATG (start codon) were extracted by TBtools. Then, the PlantCARE program (http://bioinformatics.psb.ugent.be, accessed on 15 May 2025) was used to analyze the cis-acting elements within it. The predicted cis-acting elements were screened, quantified, and categorized into four groups (elements related to biotic and abiotic stress, light-responsive elements, hormone-related elements, and elements associated with plant growth and development) using Microsoft Excel (version 2023), followed by graphical representation.

2.7. RNA Extraction and Transcriptome Analysis

Total RNA was extracted from each sample using TRIzol reagent (Invitrogen, Carlsbad, CA, USA), following the manufacturer's protocol. The quality, concentration, and integrity of RNA were detected using an Agilent 2100 Bioanalyzer (Agilent, Santa Clara, CA, USA). High-quality RNAs were subjected to construct a cDNA library using the Genomic LT-Sample Prep Kit (Illumina, San Diego, CA, USA). The cDNA libraries were sequenced as 150-mers using the Illumina HiSeq 4000 platform (Illumina Inc., San Diego, CA, USA), with three biological replicates. Reads were cleaned by removing adapter sequences, low-quality, and ambiguous regions, followed by de novo assembly using Trinity software (version 2.15.1). The thresholds for significantly differential gene expression were defined as p-value ≤ 0.05, false discovery rate (FDR) ≤ 0.05, and $|\log_2 (\text{fold change})| > 1.0$.

2.8. NnHIPPs Expression Profiles

cDNA synthesis and genomic DNA removal were performed using the All-in-One First-Strand cDNA Synthesis SuperMix for qPCR (TransGen, Beijing, China). The expres-

sion profiles of *NnHIPPs* in leaves and roots under Cd stress were quantified by qRT-PCR, using *NnActin* as the reference sequence. qRT-PCR assays were prepared by the SYBR Premix Ex Taq™ II kit (Takara, Dalian, China) in a 7500 Real-Time PCR System (Applied Biosystems, Carlsbad, CA, USA). PCR programs were performed as the following: 95 °C for 30 s; then proceeded with 40 circles of 95 °C for 10 s and 60 °C for 30 s. Relative expression levels were calculated with the $2^{-\Delta\Delta Ct}$ method. Subsequent analyses and plotting were completed using GraphPad Prism 9 software (version 9.3.1). Data analysis utilized three independent biological replicates, and statistical significance was determined by one-way ANOVA followed by Dunnett's multiple comparisons (*: $p < 0.05$; **: $p < 0.01$). All primers are detailed in Table S1.

2.9. Subcellular Localization of NnHIPP Genes

Based on the genome database of *Nelumbo nucifera* [38], specific primers (Table S1) were designed to amplify the *NnHIPP* ORFs sequences (excluding a stop codon). The resulting fragments were subsequently cloned into the pCAMBIA1305 vector, with eGFP driven by the CaMV 35S promoter using recombinant technology. The pCAMBIA1305 and pCAMBIA1305-*NnHIPP* were transformed into *Agrobacterium tumefaciens* strain EHA105. Positive clones were selected and subsequently infiltrated into leaves of five-week-old *N. benthamiana* for transient expression. GFP fluorescence signals were observed 48 to 72 h after infiltration through confocal laser scanning (LSM780: Zeiss, Oberkochen, Germany).

2.10. Heterologous Expression of the NnHIPPs in Yeast

The ORF of *NnHIPPs* were cloned into pYES2 vector (Weidi Biotechnology Co., Ltd., Shanghai, China) using specific primers outlined in Table S1, resulting in the construction of the pYES2-*NnHIPPs* plasmid. The pYES2 and pYES2-*NnHIPPs* were transformed into yeast Cd-sensitive mutant strain *ycf1*. Yeast cells were transformed via the LiOAc/PEG protocol [39]. Yeast wild-type BY4741, mutant strain *ycf1*, and *ycf1* harboring *NnHIPPs* were diluted to four concentrations: OD600 = 1.0, 0.1, 0.01, and 0.001. Three microliters of each yeast cell dilution were deposited onto SD-Ura medium (pH 5.8) containing $CdCl_2$ at concentrations of 0, 40, and 80 μM and 2% galactose [40]. Yeast cells were cultivated at 30 °C for 2–3 days, and then cell growth under both control and Cd-stress conditions was documented.

3. Results

3.1. Identification and Characteristics of NnHIPP Genes

Genome-wide analysis identified 33 *NnHIPP* genes in *Nelumbo nucifera*, characterized by the conserved CysXXCys motif in their HMA domains and C-terminal CaaX isoprenylation motifs. These genes were systematically named *NnHIPP1* to *NnHIPP33* according to their physical positions on chromosomes (Figure S1). Chromosomal distribution analysis revealed an uneven genomic arrangement, with Chromosome 1 harboring the highest number of *NnHIPP* genes (ten genes), followed by Chromosomes 3 and 4 (seven genes each). Notably, no *NnHIPP* genes were mapped to Chromosomes 7 and 8.

Bioinformatic characterization of the 33 NnHIPP proteins revealed substantial physicochemical diversity (Table S2). Protein lengths spanned 109–495 amino acids, corresponding to molecular weights of 11.99 kDa (NnHIPP28) to 52.12 kDa (NnHIPP26). Theoretical pI values ranged from 4.88 (NnHIPP33) to 9.54 (NnHIPP22), with the majority (22 of 33) classified as alkaline proteins (pI > 7). The aliphatic index varied between 36.82 (NnHIPP18) and 90 (NnHIPP10). Instability coefficients ranged between 16.08 (NnHIPP28) and 70.39 (NnHIPP07), among which 15 NnHIPPs were all below 40, including NnHIPP10 and NnHIPP23, indicating that they were all classified as stable proteins in computational predictions. The GRAVY value of all NnHIPPs was less than 0, indicating that all NnHIPPs

were predicted to be soluble proteins. Subcellular localization analysis predicted that 16 NnHIPP proteins were located in the nucleus, followed by 9 proteins each in both the nucleus and cytoplasm.

3.2. Protein Domains and Phylogenetic Analysis of NnHIPP Proteins

To elucidate the evolutionary relationships among HIPP proteins across species, we constructed a phylogenetic tree using MEGA 7.0, integrating the HMA domains (PF00403) of 33 NnHIPPs, 45 AtHIPPs, and 59 OsHIPPs (Figure 1). The resulting phylogeny classified the NnHIPP family into five distinct subfamilies (I–V), each containing 12, 7, 4, 6, and 4 members, mirroring the grouping patterns observed in both rice and Arabidopsis. Close evolutionary relationships among NnHIPP members within each subfamily suggest conserved functional roles.

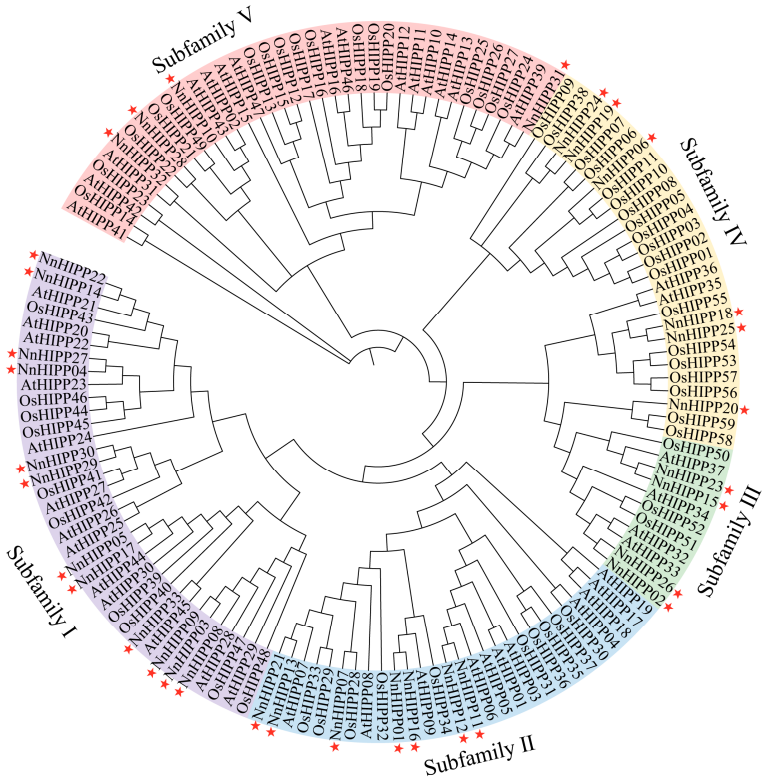

Figure 1. The phylogenetic tree of HIPP proteins from different species. Species abbreviation: Os, *Oryza sativa*; At, *Arabidopsis thaliana*; Nn, *Nelumbo nucifera*. The phylogenetic tree was constructed with the Neighbor-Joining (NJ) method (bootstrap value: 1000). The final phylogenetic tree grouped the sequences into five subfamilies, designated I–V. The red pentagrams indicate the lotus HIPP proteins.

MEME analysis identified ten conserved motifs in NnHIPP proteins, with motif 3 presented in all members (Figure 2). Sequence analysis confirmed motif 2 corresponded to the HMA domain (forming βαββαβ structures for metal binding) and motif 3 represented the C-terminal CaaX motif. Subfamily II uniquely contained four members with two HMA domains, while other subfamilies possessed single HMA domains. Distinct motif patterns characterized each subfamily: subfamily II exclusively contained motif 9, subfamily III uniquely possessed motifs 8/10 (along with longer protein lengths). The motif 5 and motif 6 were presented in both subfamily I and subfamily IV, and *NnHIPPs* in subfamily I and subfamily V were the shortest. Gene structure analysis revealed subfamily II members typically contained more exons (3–5) compared to other subfamilies (1–3 exons). Collectively, *NnHIPPs* within the same subfamily displayed similar gene structures, but differences were also revealed among various subfamilies.

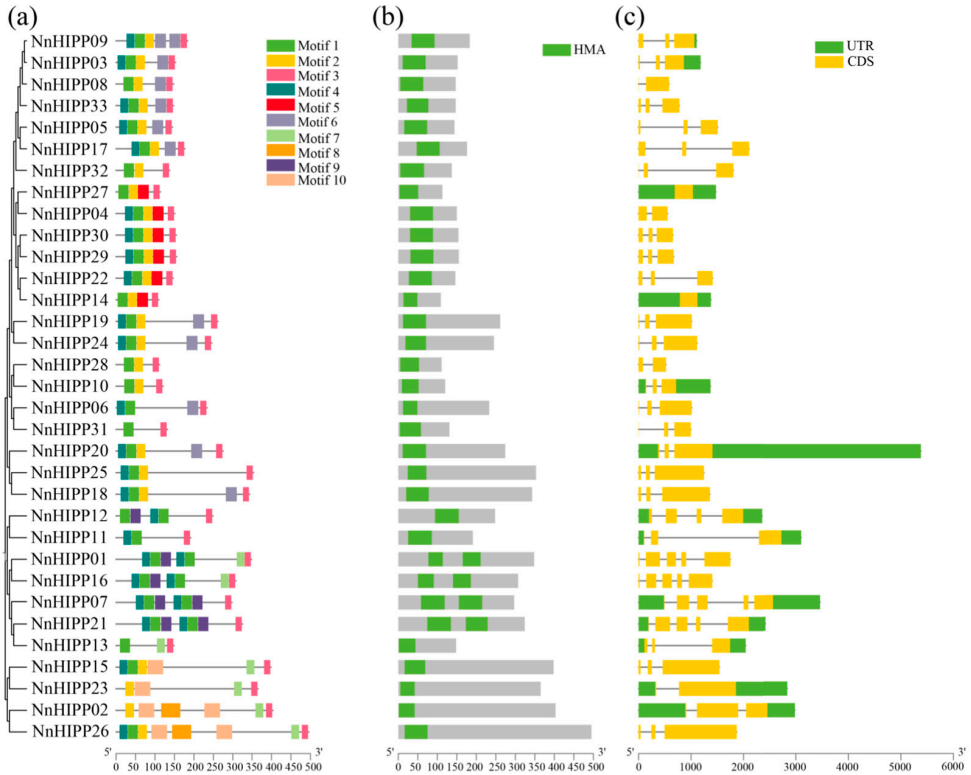

Figure 2. Phylogenetic relationships and gene structure of *NnHIPP* genes. (**a**) The systematic developmental relationship of NnHIPPs and conserved motifs of NnHIPP proteins in *Nelumbo nucifera*. A total of 10 motifs are represented by distinctly colored boxes. Gray lines denote non-conserved sequences. (**b**) Conserved domain of NnHIPP proteins. The green boxes represent the conservative HMA domain. (**c**) Intron/exon structures of *NnHIPP* genes. Exons are depicted as yellow boxes, while introns are shown as gray lines. Untranslated regions (UTRs) are represented by green boxes.

3.3. Synteny Analysis in HIPP Genes

Analysis of gene duplication events revealed nine segmental duplications within the *NnHIPP* family. Only one tandem duplication pair (*NnHIPP08*/*NnHIPP09*) was identified (Figure 3a). Furthermore, 6 and 7 collinear gene pairs were identified between lotus *HIPP* and the monocots rice and maize, respectively, while 15 and 21 synteny genes were detected in dicot *Arabidopsis* and *M. sativa* (Figure 3b). We found lotus shared significantly more conserved syntenic *HIPP* genes with dicots than with monocots. This demonstrates that *NnHIPP* genes have closer evolutionary relationships within dicots.

3.4. Cis-Regulatory Elements in the Promoters of NnHIPP Genes

Prediction of cis-acting elements in the promoter region of *NnHIPPs* can help us to explore and understand the transcriptional regulation mechanisms of *HIPPs* in lotus. Sequences 2000 bp upstream of the translation initiation site of NnHIPP genes were analyzed using the PlantCARE database (Figure 4). A total of 1788 cis-elements were identified, including 21 types of cis-regulatory elements, which were classified into four categories: 974 (54.5%) elements related to biotic and abiotic stress, 427 (23.9%) light-responsive elements, 220 (12.3%) hormone-related elements, and 167 (9.3%) elements associated with plant growth and development. Notably, each *NnHIPP* contained 4–25 MYB-recognition sites. Except for *NnHIPP05*, other *NnHIPPs* all contained 1–8 MYC-binding sites. In addition to MYB and MYC, the stress response element (STRE) and anaerobic inducing element (ARE) emerged as the most prevalent abiotic and biotic stress elements in *NnHIPP* genes. In terms of hormone-related elements, abscisic acid-responsive element (ABRE),

methyl jasmonate response elements (TGACG-motif and CGTCA-motif), salicylic acid response elements (TCA-element), and ethylene-responsive element (ERE) were identified in 33 NnHIPP genes. Additionally, various light response elements were retrieved from NnHIPP genes, including G-Box, Box 4, CAT-box, GATA-motif, GT1-motif, and TCT-motif. Further, cis-acting element analysis revealed a small number of elements related to plant growth and development, such as AAGAA-motif, as-1, CCGTCC-motif, and O2-site.

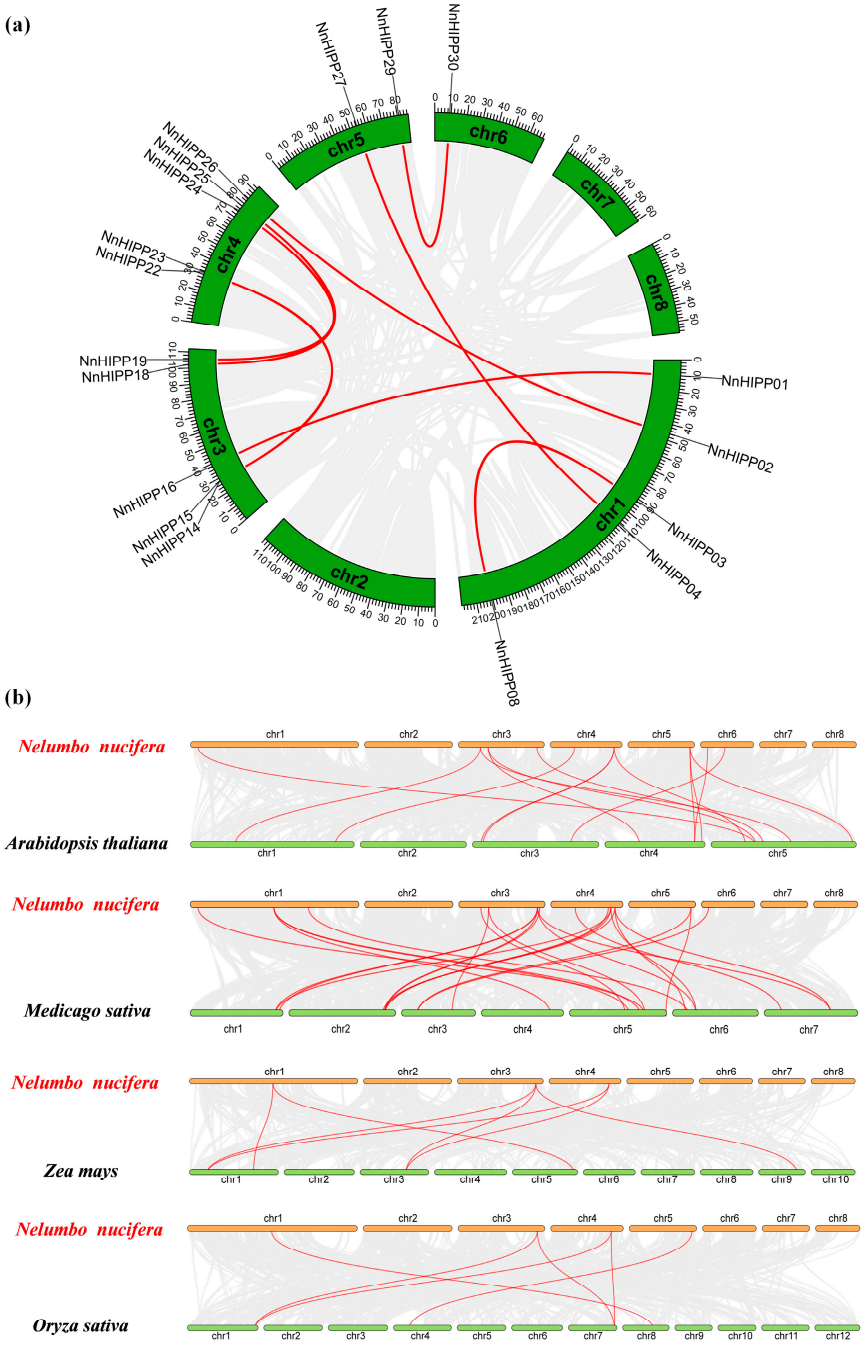

Figure 3. Gene duplication and synteny analysis of *NnHIPP* genes pairs among *Nelumbo nucifera* and four other species. (**a**) Synteny analysis of the *NnHIPP* genes in *Nelumbo nucifera*. Gray lines represent all the collinear blocks in the genome of *Nelumbo nucifera*, whereas red lines highlight duplicated *NnHIPP* pairs. (**b**) Synteny of *NnHIPP* genes with *Arabidopsis thaliana*, *Zea mays*, *Oryza sativa*, and *Medicago sativa*. Gray lines denote syntenic blocks between the two genomes, and red lines indicate collinear *NnHIPP* gene pairs. Each horizontal bar, labeled with its chromosome number below, represents a distinct chromosome.

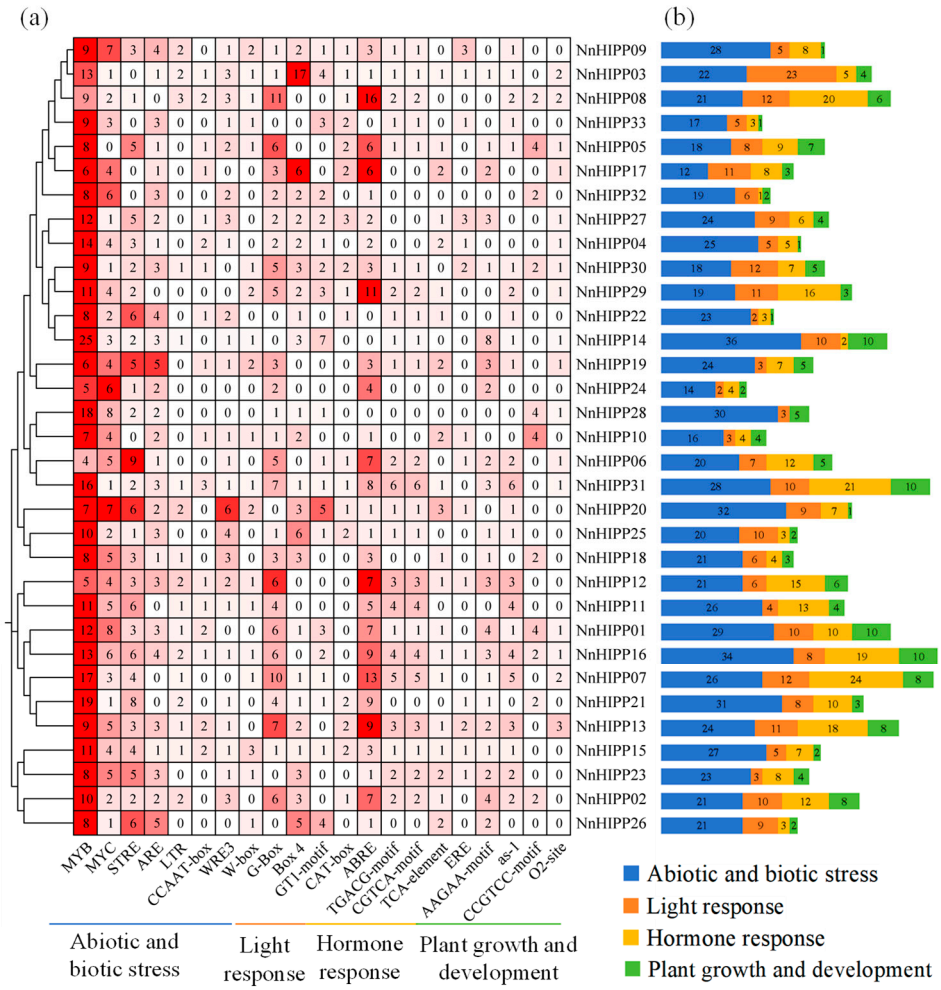

Figure 4. Identification of cis-acting elements in the *NnHIPPs* promoter regions. (**a**) Four classes of cis-acting elements in *NnHIPPs*. Grids of varying colors and numbers display the abundance of each cis-element in these *NnHIPPs*. (**b**) Histogram of adjacent cis-acting elements within each *NnHIPP* gene. The blue rectangle represents abiotic and biotic stress responsive cis-elements, orange rectangle indicates light response responsive cis-elements, yellow rectangle represents hormone response responsive cis-elements, and the green rectangle represents plant growth and development responsive cis-elements.

3.5. Expression Profiling of NnHIPP Genes in Different Tissues

To investigate the tissue-specific expression patterns of 33 *NnHIPP* genes, transcript abundances were analyzed in 16 lotus tissues and organs. As showed in Figure 5, *NnHIPP02*, *NnHIPP11*, *NnHIPP13*, *NnHIPP19*, *NnHIPP27*, and *NnHIPP31* showed relatively high expression levels in all tested tissues and developmental periods with $\log_2$FPKM > 1 (Fragments Per Kilobase of transcript per Million mapped reads), indicating that the six *NnHIPP* genes were constitutively expressed and played an essential role in the growth of lotus. Additionally, some *NnHIPP* genes exhibited a tissue-specific expression pattern. For instance, *NnHIPP28*, *NnHIPP08*, *NnHIPP06*, and *NnHIPP05* only displayed high expression levels in roots, and *NnHIPP33*, *NnHIPP04*, *NnHIPP29*, *NnHIPP31*, *NnHIPP24*, and *NnHIPP20* were highly expressed in rhizome internodes, while *NnHIPP30* was only highly expressed in leaves. *NnHIPP23* and *NnHIPP21* were highly expressed in tissues other than rhizome internodes, while *NnHIPP17* and *NnHIPP20* were expressed in tissues other than cotyledons.

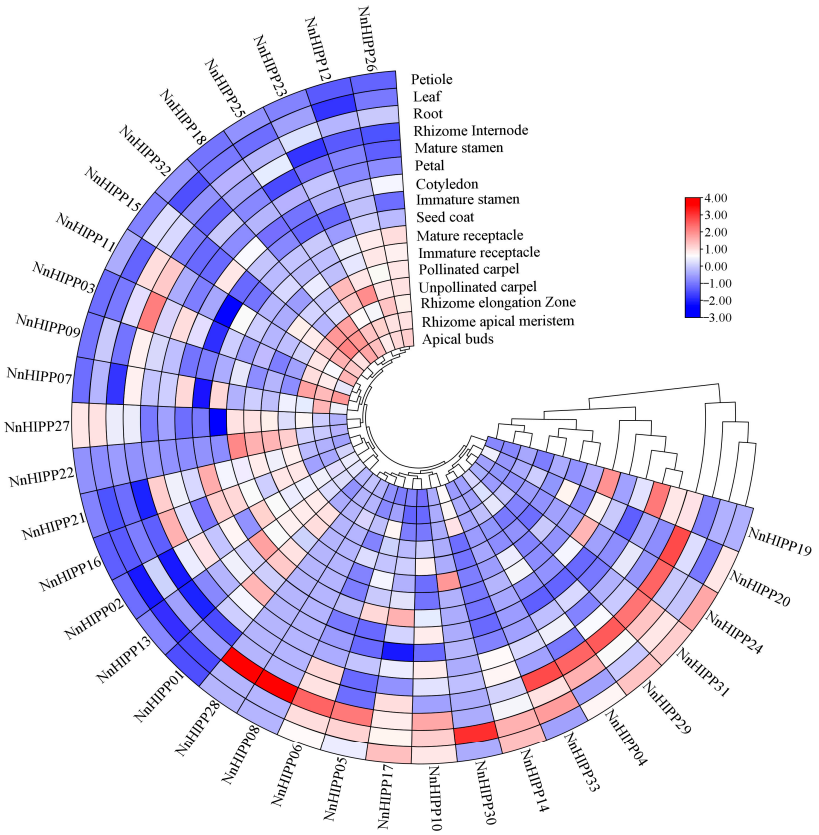

Figure 5. Expression patterns of *NnHIPP* genes across various tissues and developmental stages. The heatmap displays expression levels across 16 tissues, with seed coat and cotyledon samples sampled at 18 and 15 days post-pollination (DAP), respectively. The expression pattern was constructed using $\log_2$ (FPKM+1) values and performed with hierarchical clustering. High and low transcript accumulations are shown in red and blue, respectively, and the median level is indicated in white.

3.6. Expression Levels of NnHIPP Genes in Lotus Under Cd Stress

Previous studies have showed that *HIPP* genes are involved in the heavy metal signaling pathways and are induced by Cd stress [41,42]. When 14-day lotus seedlings were subjected to Cd stress for six and 12 h, we collected root and leaves separately, and subsequently performed transcriptome sequencing. The differentially expressed genes obtained from transcriptome analysis were screened, and *NnHIPP* genes with different response patterns were identified. As seen in Figure 6, *NnHIPP08* and *NnHIPP28* were only negatively induced by Cd stress in roots, which was consistent with their expression only in roots. With the application of excessive Cd, the expression levels of *NnHIPP13*, *NnHIPP14*, *NnHIPP15*, *NnHIPP21*, *NnHIPP23*, *NnHIPP32*, and *NnHIPP33* in both roots and leaves continued to decrease, while *NnHIPP07*, *NnHIPP20*, *NnHIPP25*, and *NnHIPP30* were continuously negatively induced only in roots. Meanwhile, *NnHIPP03*, *NnHIPP29*, and *NnHIPP31* in leaves and roots were, respectively, continuously positively induced by Cd stress. The expression levels of *NnHIPP04* and *NnHIPP27* were induced to continuously increase only in leaves, while the expression levels of *NnHIPP10* and *NnHIPP20* continuously increased only in roots. The heat map in Figure 6 revealed the majority of *HIPP* gene members were induced to express at much higher levels in the underground part than in leaves.

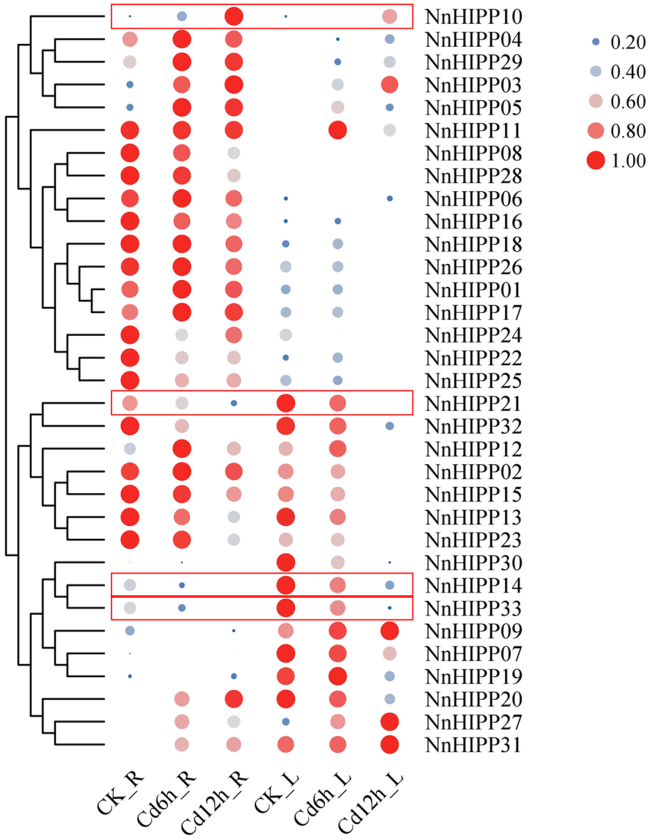

Figure 6. Expression analysis of *NnHIPPs* in *Nelumbo nucifera* under Cd treatment. R, roots; L, leaves. Cd6h/Cd12h, represents the sample treated with cadmium for 6/12 h; CK as the control. Blue and red represent lower and higher transcript abundance, respectively, compared to the control (CK_R).

Based on the expression pattern above, nine candidate genes were selected to probe the transcript abundance patterns of *NnHIPP* genes under Cd stress. We performed RT-qPCR analysis on the last fully expanded leaves and corresponding roots of *N. nucifera* under simulated Cd stress. The findings demonstrated that expression patterns of the nine genes were consistent with the transcriptome data (Figures 7 and 8). We found the response of *NnHIPP* genes was different to Cd treatment. Among the nine *NnHIPP* genes, only *NnHIPP10* and *NnHIPP27* were upregulated in leaves. Notably, the largest increase in expression was detected for *NnHIPP10*, which was 17 times more than the control in leaves. The expression level of the other seven *NnHIPP* genes (*NnHIPP21*, *NnHIPP33*, *NnHIPP20*, *NnHIPP12*, *NnHIPP23*, *NnHIPP25* and *NnHIPP14*) were decreased after Cd treatment. And *NnHIPP33* showed significantly lower expression than that in CK by Cd stress from 6 h to 48 h (Figure 7). By contrast, only *NnHIPP33* and *NnHIPP14* were downregulated after 6 h in roots (Figure 8). However, *NnHIPP21*, *NnHIPP10*, *NnHIPP27*, *NnHIPP20* and *NnHIPP12* were induced positively to different extent. *NnHIPP23* and *NnHIPP25* showed a similar pattern in that they were downregulated first at 12 h and 3 h, respectively. Then they were upregulated at 24 h and 48 h. In roots and leaves, some *NnHIPP* genes showed different expression patterns at 24 h and 48 h from other time points, such as *NnHIPP21* in leaves and *NnHIPP33* in roots. This expression pattern may be related to the wrinkling of leaves after 48 h of treatment (Figure S2). We found more *NnHIPP* genes were induced positively in roots compared in leaves, and the multiple of the induced expression in roots was much higher than that in leaves. Moreover, both *NnHIPP10* and *NnHIPP27* were upregulated after treatment in roots and leaves, and *NnHIPP10* had a stronger response intensity. Conversely, *NnHIPP33* and *NnHIPP14* were repressed after Cd treatments. Finally, almost all *NnHIPP* genes were induced after 6 h of the treatment.

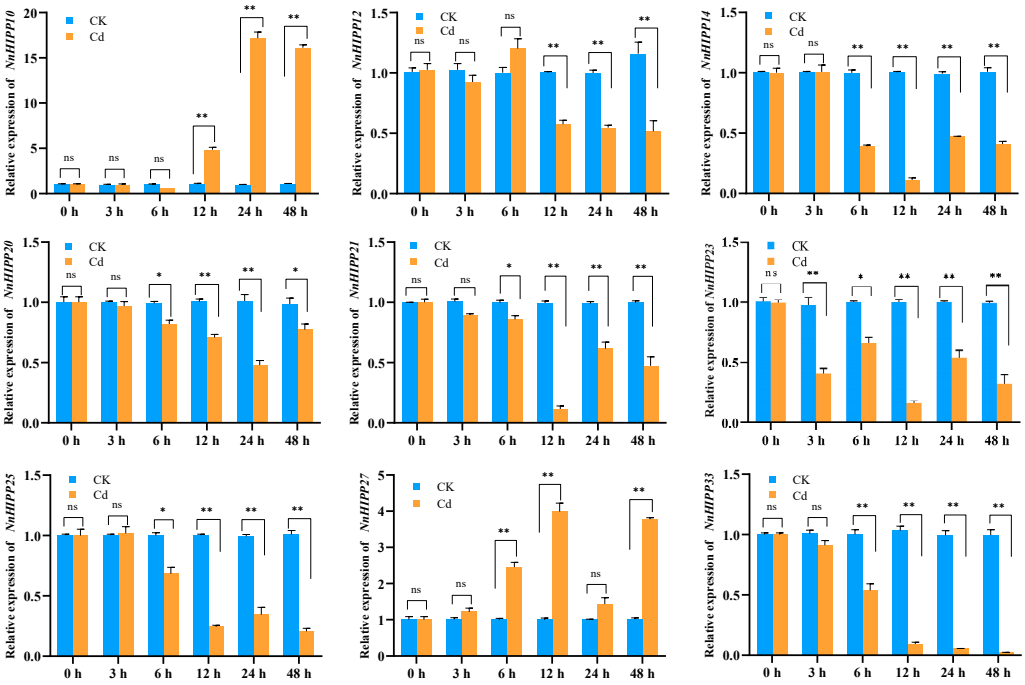

Figure 7. The expression profiles of nine representative *NnHIPP* genes in leaves of *Nelumbo nucifera* under Cd treatment were analyzed by RT-qPCR. Data presented are means ± SEM values from three independent biological replicates and three technical replicates. Statistical significance was determined by one-way ANOVA followed by Dunnett′s multiple comparisons (*: $p < 0.05$; **: $p < 0.01$). "ns" means no significant difference.

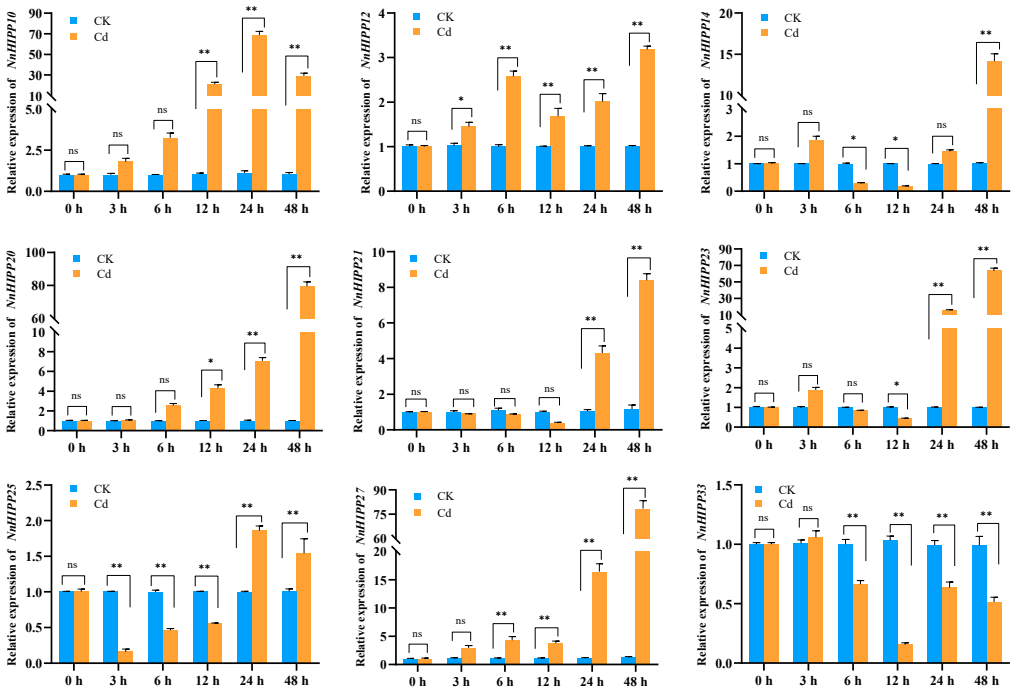

Figure 8. The expression profiles of nine representative *NnHIPP* genes in roots of lotus under Cd treatment were analyzed by RT-qPCR. Data presented are means ± SEM values from three biological replicates and three technical replicates. Statistical differences were assessed using one-way ANOVA followed by Dunnett's multiple comparison test (*: $p < 0.05$; **: $p < 0.01$). "ns" means no significant difference.

3.7. Subcellular Localization of NnHIPP Proteins

Investigating the protein localization within cells provides clues towards the elucidation of the functions and mechanisms of the genes. According to the expression pattern analysis in different tissues and RT-qPCR results under Cd stress, we selected NnHIPP10, NnHIPP14, NnHIPP21, and NnHIPP33 as candidates for further analysis. Subcellular localization of the NnHIPP-GFP fusion proteins transiently expressed in tobaccos was observed by using laser scanning confocal microscopy. The results in Figure 9 showed that the four NnHIPP proteins were all found in the plasma membrane (PM) and nucleus, although they exhibited varying levels of fluorescence intensities, e.g., the green fluorescence signals of NnHIPP14 were weaker in the plasma membrane than those of the others. In contrast, the control GFP protein was evenly distributed throughout the entire cell. These findings revealed that the four NnHIPP proteins were likely located in both plasma mem brane and nucleus. These results were partially consistent with the predictions mentioned above (Table S2).

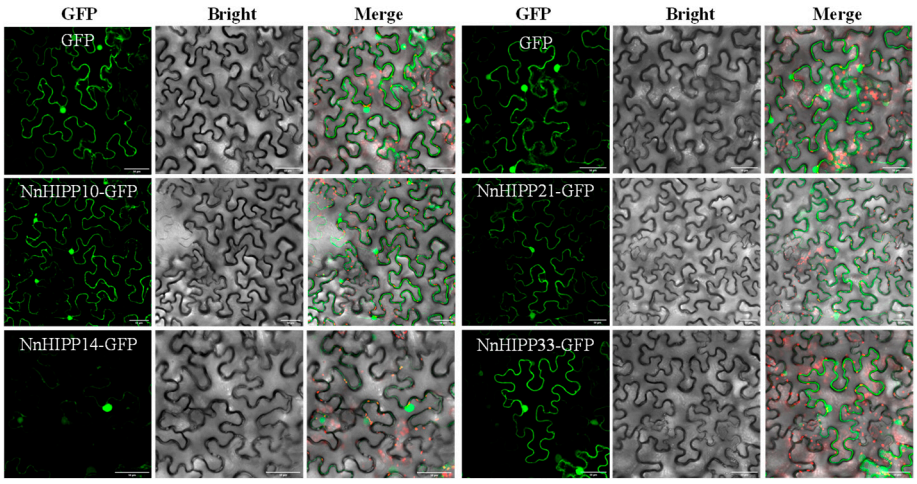

Figure 9. Subcellular localization of NnHIPP10, NnHIPP14, NnHIPP21, and NnHIPP33 fusion transgene in leaf epidermal cells of tobacco (*N. benthamiana*). GFP: the green fluorescence channel images; Bright: bright field; Merged: overlapped images of GFP and Bright. Bars = 50 μm.

3.8. The Function of NnHIPPs on Cd Tolerance in Yeast

In our previous studies, it was found that some *NnHIPPs* can be induced to express by Cd. In order to further investigate the physiological function of the *NnHIPP* genes under Cd stress, the CDS sequences of full-length *NnHIPP10*, *NnHIPP14*, *NnHIPP21*, and *NnHIPP33* were ligated to the yeast expression vector pYES2. The empty vector and ligated vectors were then transformed into wild-type *Saccharomyces cerevisiae* strain BY4714 and Cd-sensitive mutant *ycf1*, respectively. These strains were then inoculated on Cd-free (Control) and Cd-treated (40, 80 μM) media and incubated at 30 °C for 3 days to observe the cells' growth. As shown in Figure 10, in SD-URA medium without Cd stress, the WT BY4741 or mutant *ycf1* showed similar growth status. However, when cultured in medium supplemented with 40 μM or 80 μM $CdCl_2$, *ycf1* cells expressing *NnHIPP14*, *NnHIPP21*, or *NnHIPP33* demonstrated significantly enhanced growth compared to empty vector controls. The mutant strains expressing *NnHIPP10* showed similar growth with the empty vector. The growth status of transforming yeast can reflect the tolerance of *NnHIPP* genes to Cd stress. Findings revealed that *NnHIPP21* and *NnHIPP33* had comparable tolerance to Cd. *NnHIPP14* showed higher tolerance to Cd in growth status compared to *NnHIPP21* or *NnHIPP33*, while *NnHIPP10* was the gene most sensitive to Cd among the four *NnHIPP* genes.

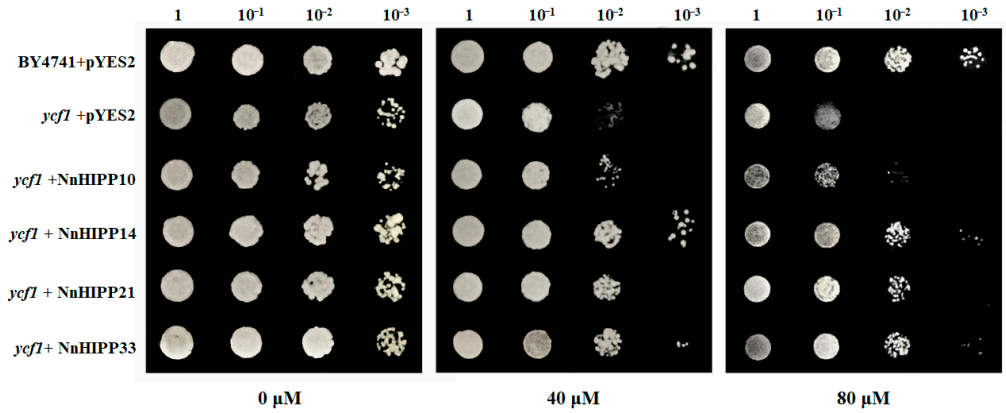

Figure 10. Cd tolerance assay in yeast. The growth of pYES2 (empty vector) transformed into yeast wild-type BY4741 and Cd-sensitive mutant ycf1 were used as positive and negative controls, respectively. Growth of *ycf1* transformed with *NnHIPP10* (*ycf1* + *NnHIPP10*), *NnHIPP14* (*ycf1* + *NnHIPP14*), *NnHIPP21* (*ycf1* + *NnHIPP21*), and *NnHIPP33* (*ycf1* + *NnHIPP33*) was assessed. The yeast phenotype under Cd treatment: 40, 80 μM $CdCl_2$, pH = 5.8, 2% galactose.

4. Discussion

Throughout evolution, plants have developed comprehensive mechanisms for heavy metal transport and detoxification. These processes involve multiple protein components, with HIPP family members serving as key mediators [43]. However, the comprehensive identification of NnHIPPs in lotus has not been achieved. This study identified 33 *NnHIPP* genes in *Nelumbo nucifera* and classified them into five distinct subfamilies through phylogenetic analysis. Notably, this pattern of classification is conserved across diverse plant species. For instance, recent studies have reported the identification of 26, 45, 23, 56, and 66 HIPP genes in *Citrus sinensis*, *Sorghum bicolor*, *Medicago sativa*, *Camellia sinensis*, and *Zea mays* [19,22–24,44]. *HIPP* genes within the same subfamily exhibit similar gene structures/lengths, and those containing two HMA domains were clustered into a single subfamily.

Gene duplication is a key mechanism by which many genes evolve novel functions, enabling plants to continuously adapt to changing environmental conditions. Gene duplication events, including tandem and segmental duplications, play a crucial role in the expansion and reorganization of the *HIPP* gene family in the lotus genome [45]. Evolutionary analysis revealed that the *NnHIPP* family expanded primarily through segmental duplication (nine pairs), as evidenced by only one tandem duplication event identified. This tandem pair (NnHIPP08/NnHIPP09) is located on Chromosome 2, which exhibits the highest *HIPP* gene density (30.3%), implicating it as a potential evolutionary hotspot for gene expansion. Furthermore, interspecies collinearity analysis showed a stronger synteny between lotus HIPPs and dicots (Arabidopsis and alfalfa) than with monocots (rice and sorghum), which is consistent with a post-divergence expansion of the family. Specific genes, such as *NnHIPP18*, *NnHIPP25*, and *NnHIPP26*, exhibited 2–4 syntenic pairs across these species, underscoring their potential evolutionary significance in the diversification of the *NnHIPP* family.

A significant proportion of cis-acting elements identified in the *NnHIPPs* promoters were associated with biotic and abiotic stress responses (54.5%), indicating that NnHIPPs play important roles in adversity adaptation. Among various cis-acting elements, MYB-binding sites were the most abundantly enriched across all genes. Notably, *NnHIPP14* and *NnHIPP21*, which are central to our follow-up investigation, contained the highest numbers of MYB-binding sites (25 and 19, respectively), suggesting that *NnHIPPs* expression may be regulated by MYB-type transcription factors. ABRE elements were also present in high numbers in most *NnHIPPs* promoters, implying potential ABA-mediated transcriptional

regulation. Previous studies have shown that elevated ABA levels reduce Cd accumulation via ABI5, which is a core ABA signaling component that interacts with MYB49 [46]. Furthermore, MYB49 directly binds to the promoters of *AtHIPP22*—a gene whose homolog in lotus is *NnHIPP14*—as well as *AtHIPP44* in Arabidopsis, upregulating their expression and enhancing Cd accumulation [28]. This conserved regulatory module suggests that *NnHIPP14* may also be regulated through MYB49-mediated mechanisms in response to Cd stress, offering a hypothesis for its role in the ABA-Cd signaling network. Further research should examine whether these MYB and ABRE elements mediate ABA-responsive regulation of *NnHIPPs* under Cd stress.

The tissue-specific and Cd-responsive expression patterns of *NnHIPP* genes provide a foundation for investigating their roles in lotus metal homeostasis. The expression profiling of *NnHIPP* genes across 16 lotus tissues revealed both constitutive and tissue-specific expression patterns, suggesting diverse functional roles in plant development and organ-specific responses. Transcriptome analysis of lotus leaves and roots under 6 h and 12 h Cd exposure revealed that 29 out of 33 NnHIPP genes were differentially expressed in at least one tissue, demonstrating their widespread involvement in Cd response. The predominant positive induction of *NnHIPP* genes in roots, with higher fold-changes compared to leaves, underscores the role of roots as the primary site for metal uptake and initial detoxification. This is consistent with the physiological need for roots to rapidly absorb or exclude toxic Cd to maintain metal homeostasis [47,48]. *NnHIPP10* was strongly upregulated, especially in roots, suggesting its role in early metal sequestration. In contrast, *NnHIPP14* and *NnHIPP21* displayed distinct tissue-specific patterns—decreasing in leaves but increasing in roots over time—implying their potential involvement in Cd trafficking or tolerance mechanisms. Conversely, *NnHIPP33* was downregulated in both tissues. Collectively, these results highlight the functional diversification of *NnHIPP* genes in mediating Cd uptake, translocation, and detoxification, with roots serving as a critical frontline barrier against metal toxicity.

The isoprenylation motif in HIPPs mediates specific interactions with endomembrane systems or transport proteins, thereby modulating protein localization [6,22]. Subcellular localization analysis showed that NnHIPP10, NnHIPP14, NnHIPP21, and NnHIPP33 are located at the plasma membrane and in the nucleus. Since these proteins lack transmembrane domains, we propose that NnHIPPs may facilitate Cd detoxification at the membrane–cytoplasm interface. Upon entering the cytoplasm, Cd may be captured by membrane-anchored NnHIPPs to form protein–Cd complexes. Through the isoprenyl group, these complexes may then interact specifically with Cd efflux transporters, such as OsZIP1, OsABCG36, or OsHMA9 [49–51], to transfer Cd for extrusion, thereby reducing intracellular Cd accumulation and alleviating toxicity. While this proposed mechanism aligns with established roles of HIPPs in metal detoxification [18,19,22,25,26,42,52,53], the additional nuclear localization of some NnHIPPs further suggests potential roles in metal-responsive transcriptional regulation or signaling, highlighting the multifunction of NnHIPP10/14/21/33. Further validation through detailed co-localization studies using organelle-specific markers and functional transport assays is essential.

Functional analysis using a heterologous yeast expression system demonstrated that overexpression of NnHIPP14, NnHIPP21, and NnHIPP33 significantly enhanced Cd tolerance in the sensitive *ycf1* mutant, indicating their potential role in heavy metal detoxification. Among these, NnHIPP14 conferred the strongest tolerance, followed by NnHIPP21 and NnHIPP33, whereas NnHIPP10 did not improve growth under Cd stress, suggesting functional divergence within the NnHIPP family. These results align with previous studies showing that Arabidopsis homologs AtHIPP20, AtHIPP22, AtHIPP26, and AtHIPP27—which belong to the same subfamily I as NnHIPP14 and NnHIPP33—also enhance Cd tolerance in yeast [41].

Furthermore, AtHIPP26 (AtFP6) was reported to improve Cd tolerance in transgenic plants by mitigating oxidative stress [54]. The conserved function of subfamily I members across species highlights their evolutionary importance in metal homeostasis. Previous studies reported that cysteine residues within HMA domains serve as potential metal-binding sites, mediating heavy metal sequestration to mitigate cellular toxicity [55,56]. Notably, NnHIPP21 contains two HMA domains, which may enhance its capacity to bind Cd and facilitate detoxification. However, the inability of NnHIPP10 to confer resistance underscores the necessity of selecting appropriate candidates for genetic engineering aimed at improving metal tolerance. Further studies in lotus are needed to validate the efficacy and mechanistic roles of NnHIPP14, NnHIPP21, and NnHIPP33 in Cd detoxification.

Cd is a highly soluble and extremely toxic heavy metal that poses a serious threat to living organisms and ecosystems. It readily accumulates in aquatic environments and enters plants through nutrient transport pathways, causing severe cellular damage and oxidative stress [4,40]. Due to its high mobility and bioavailability in water, Cd-contaminated aquatic systems present particularly urgent ecological and health risks. Therefore, effective removal of Cd from water is essential to mitigate its harmful impact. Phytoremediation is an environmentally sustainable approach that utilizes specially selected or genetically enhanced plants to absorb, sequester, and detoxify cadmium from contaminated water, thereby reducing ecological risks and restoring water quality. Studies on Cd-stress response in aquatic plants have revealed multiple gene families contributing to Cd detoxification, accumulation, and tolerance, including glutathione-dependent SpGSH1 (glutamate-cysteine ligase) and SpPCS1 (phytochelatin synthase), SpNRAMP (natural resistance-associated macrophage proteins) transporters SpNramp1/2/3 in *Spirodela polyrhiza*, and glutathione S-transferase gene *LmGSTF3* in *Lemna minor* [40,57–59]. In *Nelumbo nucifera*, several transcription factor families have been identified as key regulators in the response to Cd stress, like brassinazole-resistant (BZR) transcription factors (particularly NnBZR1.2), ethylene-responsive factors (ERFs), and Q-type C2H2 zinc finger proteins (ZFPs) [30,60,61]. Our study identified and functionally characterized heavy metal chaperone proteins from the NnHIPP family in lotus, ultimately screening three candidate genes (NnHIPP14/21/33) with enhanced potential for Cd tolerance and accumulation. Future work will focus on validating the Cd sequestration functions of NnHIPPs through transgenic studies and assess the remediation potential of high-accumulating lotus varieties, aiming to develop effective phytoremediation strategies for water purification.

5. Conclusions

This study provides the first genome-wide functional characterization of the *HIPP* gene family in *Nelumbo nucifera*, revealing its structural, evolutionary, and functional characteristics in response to Cd stress. A total of 33 *NnHIPP* genes were identified, all containing conserved metal-binding HMA and C-terminal prenylation motifs, and classified into five phylogenetic subfamilies with distinct motif compositions and gene structures. The *NnHIPP* genes show closer synteny with dicots than monocots, highlighting lineage-specific expansion. Their promoters contain abundant stress-responsive cis-elements, supporting involvement in transcriptional regulation under abiotic stress. Expression profiling demonstrated both tissue-specific and Cd-induced patterns, leading to the selection of four candidates (NnHIPP10/14/21/33) for further functional validation. Notably, NnHIPP14, NnHIPP21, and NnHIPP33 confer enhanced Cd tolerance in transgenic yeast and exhibit dual localization in the nucleus and plasma membrane, supporting their role in metal ion homeostasis. These findings not only elucidate the functional diversification of *NnHIPP* genes in Cd adaptation, but also provide valuable genetic targets for developing Cd-tolerant lotus varieties to enhance phytoremediation efficiency in heavy-metal-contaminated aquatic environments.

Supplementary Materials: The following supporting information can be downloaded at https://www.mdpi.com/article/10.3390/horticulturae11091136/s1: Table S1: Primers used in qRT-PCR; Table S2: The sequence information and physicochemical properties of NnHIPPs; Figure S1: The distribution map of *NnHIPP* genes on the six chromosomes of lotus; Figure S2: The phenotype of lotus leaves after 48 h of cadmium-stress treatment.

Author Contributions: C.G.: conceptualization, methodology, formal analysis, writing—original draft, writing—review and editing; Y.Z. and H.X.: methodology, formal analysis; K.Y. and X.G.: data curation, formal analysis; X.P. and Y.X.: software, investigation; J.C.: data curation; Y.W.: methodology, formal analysis, writing—review and editing. All authors have read and agreed to the published version of the manuscript.

Funding: This work was supported by the Natural Science Key Foundations of the Anhui Bureau of Education (2024AH051452), the Biological and Medical Sciences of Applied Summit Nurturing Disciplines in Anhui Province (Anhui Education Secretary Department [2023]13), Provincial Germplasm Resource Bank Project (2024–SJ–015), Science and Technology Program of Suzhou City (SNG2022050), major research project supported by Anhui Huatuo Academy of Traditional Chinese Medicine (BZKZ2419), Student Research Project at Fuyang Normal University (XSXM24-094), and the Fuyang Normal University doctoral talent introduction project (2023KYQD0028, 2025KYQD0034).

Institutional Review Board Statement: Not applicable.

Informed Consent Statement: Not applicable.

Data Availability Statement: All raw data have been deposited in the NCBI Sequence Read Archive (SRA) under the accession number PRJNA1305686. The data presented in this study are available in the Supplementary Materials.

Acknowledgments: We thank our contributors for their dedication and compliance through the many stages of this research, as well as the editors and anonymous reviewers whose comments helped to greatly improve this paper.

Conflicts of Interest: The authors declare no conflicts of interest.

Abbreviations

The following abbreviations are used in this manuscript:

ABA	Abscisic acid
Cd	Cadmium
CDS	Coding sequences
CKX	Cytokinin oxidase
FPKM	Fragments per kilobase of transcript per million mapped reads
HIPP	Heavy metal-associated isoprenylated plant protein
HMA	Heavy metal-associated
HMM	Hidden Markov model
Pb	Lead
STRE	Stress response promoter element

References

1. Zhao, F.J.; Tang, Z.; Song, J.J.; Huang, X.Y.; Wang, P. Toxic metals and metalloids: Uptake, transport, detoxification, phytoremediation, and crop improvement for safer food. *Mol. Plant* **2022**, *15*, 27–44. [CrossRef]
2. Anwar, A.; Wang, Y.D.; Chen, M.Q.; Zhang, S.W.; Wang, J.M.; Feng, Y.Q.; Xue, Y.X.; Zhao, M.F.; Su, W.; Chen, R.Y.; et al. Zero-valent iron (nZVI) nanoparticles mediate SlERF1 expression to enhance cadmium stress tolerance in tomato. *J. Hazard. Mater.* **2024**, *468*, 133829. [CrossRef]
3. Tang, W.; Liang, L.; Yang, H.; Yu, X.; Ye, X.; Xie, Y.; Li, R.; Lin, L.; Huang, Z.; Sun, B.; et al. Exogenous salicylic acid reduces cadmium content in spinach (*Spinacia oleracea* L.) shoots under cadmium stress. *BMC Plant Biol.* **2024**, *24*, 1226. [CrossRef]
4. Hu, Y.; He, R.; Mu, X.; Zhou, Y.; Li, X.; Wang, H.; Xing, W.; Liu, D. Cadmium toxicity in plants: From transport to tolerance mechanisms. *Plant Signal. Behav.* **2025**, *20*, 2544316. [CrossRef]

5. Tang, Z.; Wang, H.Q.; Chen, J.; Chang, J.D.; Zhao, F.J. Molecular mechanisms underlying the toxicity and detoxification of trace metals and metalloids in plants. *J. Integr. Plant Biol.* **2023**, *65*, 570–593. [CrossRef] [PubMed]
6. Wu, W.; Zhao, T.; Zheng, Y.; Liu, T.; Zhou, S.; Chen, W.; Xie, L.; Lin, Q.; Chen, L.; Xiao, S.; et al. *HIPP33* Contributes to Selective Autophagy-Mediated Vacuolar Sequestration of Cadmium in Arabidopsis. *Plant Cell Environ.* **2025**, *48*, 7072–7088. [CrossRef]
7. Chen, J.; Huang, X.Y.; Salt, D.E.; Zhao, F.J. Mutation in *OsCADT1* enhances cadmium tolerance and enriches selenium in rice grain. *New Phytol.* **2020**, *226*, 838–850. [CrossRef] [PubMed]
8. Li, Y.; Rahman, S.U.; Qiu, Z.; Shahzad, S.M.; Nawaz, M.F.; Huang, J.; Naveed, S.; Li, L.; Wang, X.; Cheng, H. Toxic effects of cadmium on the physiological and biochemical attributes of plants, and phytoremediation strategies: A review. *Environ. Pollut.* **2023**, *325*, 121433. [CrossRef]
9. Yu, Y.; Alseekh, S.; Zhu, Z.H.; Zhou, K.J.; Fernie, A.R. Multiomics and biotechnologies for understanding and influencing cadmium accumulation and stress response in plants. *Plant Biotechnol. J.* **2024**, *22*, 2641–2659. [CrossRef] [PubMed]
10. Haider, F.U.; Cai, L.; Coulter, J.A.; Cheema, S.A.; Wu, J.; Zhang, R.; Ma, W.; Farooq, M. Cadmium toxicity in plants: Impacts and remediation strategies. *Ecotoxicol. Environ. Saf.* **2021**, *211*, 111887. [CrossRef]
11. Khan, A.H.A.; Kiyani, A.; Mirza, C.R.; Butt, T.A.; Barros, R.; Ali, B.; Iqbal, M.; Yousaf, S. Ornamental plants for the phytoremediation of heavy metals: Present knowledge and future perspectives. *Environ. Res.* **2021**, *195*, 110780. [CrossRef]
12. Wang, Y.; Yuan, M.; Li, Z.; Niu, Y.; Jin, Q.; Zhu, B.; Xu, Y. Effects of ethylene biosynthesis and signaling on oxidative stress and antioxidant defense system in *Nelumbo nucifera* G. under cadmium exposure. *Environ. Sci. Pollut. Res.* **2020**, *27*, 40156–40170. [CrossRef]
13. Zhou, P.; Jin, Q.; Qian, P.; Wang, Y.; Wang, X.; Jiang, H.; Yao, D.; Liu, X.; Liu, F.; Li, J.; et al. Genetic resources of lotus (*Nelumbo*) and their improvement. *Ornam. Plant Res.* **2022**, *2*, 5. [CrossRef]
14. Liu, Q.; Wang, L.; Zhang, D. Characterization of the phytochemical content, antioxidant activity and inhibition capacity against α-glucosidase of different flower parts of seven lotuses (*Nelumbo*). *Sci. Hortic.* **2023**, *316*, 112007. [CrossRef]
15. Liu, A.; Tian, D.; Xiang, Y.; Mo, H. Effects of biochar on growth of Asian lotus (*Nelumbo nucifera* Gaertn.) and cadmium uptake in artificially cadmium-polluted water. *Sci. Hortic.* **2016**, *198*, 311–317. [CrossRef]
16. Mishra, V.; Pathak, V.; Tripathi, B. Accumulation of cadmium and copper from aqueous solutions using Indian lotus (*Nelumbo nucifera*). *Ambio* **2009**, *38*, 110–112. [CrossRef]
17. de Abreu-Neto, J.B.; Turchetto-Zolet, A.C.; de Oliveira, L.F.V.; Zanettini, M.H.B.; Margis-Pinheiro, M. Heavy metal-associated isoprenylated plant protein (HIPP): Characterization of a family of proteins exclusive to plants. *FEBS J.* **2013**, *280*, 1604–1616. [CrossRef]
18. Cao, H.W.; Zhao, Y.N.; Liu, X.S.; Rono, J.K.; Yang, Z.M. A metal chaperone OsHIPP16 detoxifies cadmium by repressing its accumulation in rice crops. *Environ. Pollut.* **2022**, *311*, 120058. [CrossRef]
19. Huang, G.Y.; Hu, Y.N.; Li, F.X.; Zuo, X.R.; Wang, X.Y.; Li, F.Y.; Li, R.M. Genome-wide characterization of heavy metal-associated isoprenylated plant protein gene family from *Citrus sinensis* in response to huanglongbing. *Front. Plant Sci.* **2024**, *15*, 1369883. [CrossRef]
20. Wang, Z.K.; Zhang, H.; Li, Y.B.; Chen, Y.M.; Tang, X.; Zhao, J.; Yu, F.F.; Wang, H.Y.; Xiao, J.; Liu, J.; et al. Isoprenylation modification is required for HIPP1-mediated powdery mildew resistance in wheat. *Plant Cell Environ.* **2023**, *46*, 288–305. [CrossRef]
21. Zschiesche, W.; Barth, O.; Daniel, K.; Böhme, S.; Rausche, J.; Humbeck, K. The zinc-binding nuclear protein HIPP3 acts as an upstream regulator of the salicylate-dependent plant immunity pathway and of flowering time in *Arabidopsis thaliana*. *New Phytol.* **2015**, *207*, 1084–1096. [CrossRef] [PubMed]
22. Zhang, H.; Zhai, G.W.; Ni, X.L.; Liu, Z.W.; Song, T.; Han, Y.; Wang, Y.; Shao, Y.; Wang, F.L.; Zou, G.H.; et al. Genome-wide identification of HIPP genes family in sorghum reveals the novel role of SbHIPP40 in accumulation of cadmium. *J. Hazard. Mater.* **2025**, *494*, 138478. [CrossRef]
23. Xia, H.Y.; Jing, X.; He, H.Q.; Peng, J.W.; Liu, Y.Y.; Sun, W.Y.; Wang, X.Z.; Yuan, Z.; Wu, J.X.; Zhang, M.Y.; et al. Genome-wide identification of the HIPPs gene family and functional validation of MsHIPP12 in enhancing cadmium tolerance in *Medicago sativa*. *J. Hazard. Mater.* **2025**, *491*, 137894. [CrossRef]
24. Wei, Y.F.; Peng, X.Q.; Wang, X.J.; Wang, C. The heavy metal-associated isoprenylated plant protein (HIPP) gene family plays a crucial role in cadmium resistance and accumulation in the tea plant (*Camellia sinensis* L.). *Ecotoxicol. Environ. Saf.* **2023**, *260*, 115077. [CrossRef]
25. Ma, L.; An, R.; Jiang, L.; Zhang, C.; Li, Z.; Zou, C.; Yang, C.; Pan, G.; Lubberstedt, T.; Shen, Y. Effects of ZmHIPP on lead tolerance in maize seedlings: Novel ideas for soil bioremediation. *J Hazard Mater* **2022**, *430*, 128457. [CrossRef]
26. Zhang, B.; Liu, X.; Feng, S.; Zhao, Y.; Wang, L.; Rono, J.; Li, H.; Yang, Z. Developing a cadmium resistant rice genotype with *OsHIPP29* locus for limiting cadmium accumulation in the paddy crop. *Chemosphere* **2020**, *247*, 125958. [CrossRef]
27. Chen, G.Q.; Xiong, S. OsHIPP24 is a Copper Metallochaperone Which Affects Rice Growth. *J. Plant Biol.* **2021**, *64*, 145–153. [CrossRef]

28. Zhang, P.; Wang, R.; Ju, Q.; Li, W.; Tran, L.; Xu, J. The R2R3-MYB Transcription Factor MYB49 Regulates Cadmium Accumulation. *Plant Physiol.* **2019**, *180*, 529–542. [CrossRef]
29. Guo, T.; Weber, H.; Niemann, M.C.E.; Theisl, L.; Leonte, G.; Novak, O.; Werner, T. Arabidopsis HIPP proteins regulate endoplasmic reticulum-associated degradation of CKX proteins and cytokinin responses. *Mol. Plant* **2021**, *14*, 1918–1934. [CrossRef]
30. Liu, H.; Liu, Y.D.; Liu, F.Y.; Zeng, L.H.; Xu, Y.C.; Jin, Q.J.; Wang, Y.J. Genome-wide identification of the Q-type C2H2 zinc finger protein gene family and expression analysis under abiotic stress in lotus (*Nelumbo nucifera* G.). *BMC Genom.* **2024**, *25*, 648. [CrossRef]
31. Jin, Q.J.; Wang, Y.X.; Li, X.; Wu, S.; Wang, Y.J.; Luo, J.Y.; Mattson, N.; Xu, Y.C. Interactions between ethylene, gibberellin and abscisic acid in regulating submergence induced petiole elongation in *Nelumbo nucifera*. *Aquat. Bot.* **2017**, *137*, 9–15. [CrossRef]
32. Horton, P.; Park, K.-J.; Obayashi, T.; Fujita, N.; Harada, H.; Adams-Collier, C.J.; Nakai, K. WoLF PSORT: Protein localization predictor. *Nucleic Acids Res.* **2007**, *35*, W585–W587. [CrossRef]
33. Sievers, F.; Higgins, D.G. Clustal Omega for making accurate alignments of many protein sequences. *Protein Sci.* **2018**, *27*, 135–145. [CrossRef] [PubMed]
34. Chen, S.; Chen, W.; Liu, Y.; Ahmad, M.Z.; Feng, J.; Chen, H.; Qi, X.; Deng, Y. Overexpression of ATP binding cassette transporters (ABCs) from *Hydrangea macrophylla* enhance aluminum tolerance. *J. Hazard. Mater.* **2025**, *495*, 138988. [CrossRef]
35. Chen, C.; Chen, H.; Zhang, Y.; Thomas, H.R.; Frank, M.H.; He, Y.; Xia, R. TBtools: An Integrative Toolkit Developed for Interactive Analyses of Big Biological Data. *Mol. Plant* **2020**, *13*, 1194–1202. [CrossRef]
36. Chen, C.J.; Wu, Y.; Li, J.W.; Wang, X.; Zeng, Z.H.; Xu, J.; Liu, Y.L.; Feng, J.T.; Chen, H.; He, Y.H.; et al. TBtools-II: A "one for all, all for one" bioinformatics platform for biological big-data mining. *Mol. Plant* **2023**, *16*, 1733–1742. [CrossRef]
37. Wang, Y.P.; Tang, H.B.; Wang, X.Y.; Sun, Y.; Joseph, P.V.; Paterson, A.H. Detection of colinear blocks and synteny and evolutionary analyses based on utilization of MCScanX. *Nat. Protoc.* **2024**, *19*, 2206–2229. [CrossRef]
38. Li, H.; Yang, X.Y.; Zhang, Y.; Gao, Z.Y.; Liang, Y.T.; Chen, J.M.; Shi, T. Nelumbo genome database, an integrative resource for gene expression and variants of *Nelumbo nucifera*. *Sci. Data* **2021**, *8*, 38. [CrossRef]
39. Ma, X.; Yang, H.; Bu, Y.; Wu, X.; Sun, N.; Xiao, J.; Jing, Y. Genome-wide identification of *PLATZ* genes related to cadmium tolerance in *Populus trichocarpa* and characterization of the role of *PtPLATZ3* in phytoremediation of cadmium. *Int. J. Biol. Macromol.* **2023**, *228*, 732–743. [CrossRef] [PubMed]
40. Chen, Y.; Yang, J.J.; Zhao, X.Y.; Sun, Z.L.; Li, G.J.; Hussain, S.; Li, X.Z.; Zhang, L.Y.; Wang, Z.Y.; Gong, H.H.; et al. Effects of *SpGSH1* and *SpPCS1* overexpression or co-overexpression on cadmium accumulation in yeast and *Spirodela polyrhiza*. *Plant Physiol. Biochem.* **2024**, *216*, 109097. [CrossRef]
41. Tehseen, M.; Cairns, N.; Sherson, S.; Cobbett, C.S. Metallochaperone-like genes in *Arabidopsis thaliana*. *Metallomics* **2010**, *2*, 556–564. [CrossRef]
42. Khan, I.U.; Rono, J.K.; Liu, X.; Feng, S.; Li, H.; Chen, X.; Yang, Z. Functional characterization of a new metallochaperone for reducing cadmium concentration in rice crop. *J. Clean. Prod.* **2020**, *272*, 123152. [CrossRef]
43. Khan, I.U.; Rono, J.K.; Zhang, B.Q.; Liu, X.S.; Wang, M.Q.; Wang, L.L.; Wu, X.C.; Chen, X.; Cao, H.W.; Yang, Z.M. Identification of novel rice (*Oryza sativa*) *HPP* and *HIPP* genes tolerant to heavy metal toxicity. *Ecotoxicol. Environ. Saf.* **2019**, *175*, 8–18. [CrossRef]
44. Gao, C.; Zhang, Z.; Zhu, Y.; Tian, J.; Yu, K.; Hou, J.; Luo, D.; Cai, J.; Zhu, Y. Genome-Wide Analysis of *HIPP* Gene Family in Maize Reveals Its Role in the Cadmium Stress Response. *Genes* **2025**, *16*, 770. [CrossRef]
45. Hou, J.; Liu, M.; Yang, K.; Liu, B.; Liu, H.H.; Liu, J.Q. Genetic variation for adaptive evolution in response to changed environments in plants. *J. Integr. Plant Biol.* **2025**, *67*, 2265–2293. [CrossRef]
46. Hsu, Y.T.; Kao, C.H. Role of abscisic acid in cadmium tolerance of rice (*Oryza sativa* L.) seedlings. *Plant Cell Environ.* **2003**, *26*, 867–874. [CrossRef]
47. Miyadate, H.; Adachi, S.; Hiraizumi, A.; Tezuka, K.; Nakazawa, N.; Kawamoto, T.; Katou, K.; Kodama, I.; Sakurai, K.; Takahashi, H.; et al. OsHMA3, a P_{1B}-type of ATPase affects root-to-shoot cadmium translocation in rice by mediating efflux into vacuoles. *New Phytol.* **2011**, *189*, 190–199. [CrossRef] [PubMed]
48. Luo, J.S.; Huang, J.; Zeng, D.L.; Peng, J.S.; Zhang, G.B.; Ma, H.L.; Guan, Y.; Yi, H.Y.; Fu, Y.L.; Han, B.; et al. A defensin-like protein drives cadmium efflux and allocation in rice. *Nat. Commun.* **2018**, *9*, 645. [CrossRef]
49. Fu, S.; Lu, Y.S.; Zhang, X.; Yang, G.Z.; Chao, D.; Wang, Z.G.; Shi, M.X.; Chen, J.G.; Chao, D.Y.; Li, R.B.; et al. The ABC transporter ABCG36 is required for cadmium tolerance in rice. *J. Exp. Bot.* **2019**, *70*, 5909–5918. [CrossRef]
50. Liu, X.S.; Feng, S.J.; Zhang, B.Q.; Wang, M.Q.; Cao, H.W.; Rono, J.K.; Chen, X.; Yang, Z.M. OsZIP1 functions as a metal efflux transporter limiting excess zinc, copper and cadmium accumulation in rice. *BMC Plant Biol.* **2019**, *19*, 283. [CrossRef] [PubMed]
51. Lee, S.; Kim, Y.Y.; Lee, Y.; An, G. Rice P_{1B}-type heavy-metal ATPase, OsHMA9, is a metal efflux protein. *Plant Physiol.* **2007**, *145*, 831–842. [CrossRef] [PubMed]
52. Zhao, Y.N.; Wang, M.Q.; Li, C.; Cao, H.W.; Rono, J.K.; Yang, Z.M. The metallochaperone *OsHIPP56* gene is required for cadmium detoxification in rice crops. *Environ. Exp. Bot.* **2022**, *193*, 104680. [CrossRef]

53. Cao, H.W.; Li, C.; Zhang, B.Q.; Rono, J.K.; Yang, Z.M. A Metallochaperone HIPP33 Is Required for Rice Zinc and Iron Homeostasis and Productivity. *Agronomy* **2022**, *12*, 488. [CrossRef]
54. Gao, W.; Xiao, S.; Li, H.Y.; Tsao, S.W.; Chye, M.L. *Arabidopsis thaliana* acyl-CoA-binding protein ACBP2 interacts with heavy-metal-binding farnesylated protein AtFP6. *New Phytol.* **2009**, *181*, 89–102. [CrossRef]
55. Sun, C.J.; Yang, M.; Li, Y.; Tian, J.J.; Zhang, Y.Y.; Liang, L.M.; Liu, Z.H.; Chen, K.; Li, Y.T.; Lv, K.; et al. Comprehensive analysis of variation of cadmium accumulation in rice and detection of a new weak allele of *OsHMA3*. *J. Exp. Bot.* **2019**, *70*, 6389–6400. [CrossRef]
56. Kuramata, M.; Masuya, S.; Takahashi, Y.; Kitagawa, E.; Inoue, C.; Ishikawa, S.; Youssefian, S.; Kusano, T. Novel cysteine-rich peptides from Digitaria ciliaris and *Oryza sativa* enhance tolerance to cadmium by limiting its cellular accumulation. *Plant Cell Physiol.* **2009**, *50*, 106–117. [CrossRef]
57. Chen, Y.; Li, G.; Yang, J.; Zhao, X.; Sun, Z.; Hou, H. Role of *Nramp* transporter genes of *Spirodela polyrhiza* in cadmium accumulation. *Ecotoxicol. Environ. Saf.* **2021**, *227*, 112907. [CrossRef] [PubMed]
58. Chen, Y.; Zhao, X.; Li, G.; Kumar, S.; Sun, Z.; Li, Y.; Guo, W.; Yang, J.; Hou, H. Genome-Wide Identification of the Nramp Gene Family in *Spirodela polyrhiza* and Expression Analysis under Cadmium Stress. *Int. J. Mol. Sci.* **2021**, *22*, 6414. [CrossRef]
59. Wang, X.; Huang, J.H.; Meng, B.; Mao, K.; Zheng, M.; Tan, A.; Yang, G.; Feng, X. *LmGSTF3* Overexpression Enhances Cadmium Tolerance in *Lemna minor*. *Environ. Sci. Technol.* **2024**, *59*, 2711–2721. [CrossRef]
60. Zhou, P.; Jiang, H.; Li, J.; Jin, Q.; Wang, Y.; Xu, Y. Genome-Wide Identification Reveals That BZR1 Family Transcription Factors Involved in Hormones and Abiotic Stresses Response of Lotus (*Nelumbo*). *Horticulturae* **2023**, *9*, 882. [CrossRef]
61. Xu, Y.C.; Jiang, J.N.; Zeng, L.H.; Liu, H.; Jin, Q.J.; Zhou, P.; Wang, Y.J. Genome-wide identification and analysis of ERF transcription factors related to abiotic stress responses in *Nelumbo nucifera*. *BMC Plant Biol.* **2024**, *24*, 1057. [CrossRef]